Photoelectrocatalytic Activity of Electrosynthesised Tungsten Trioxide-Titanium Dioxide Bi-Layer Coatings for the Photooxidation of Organics

J. Georgieva[1], S. Armyanov[1], E. Valova[1], N. Phillipides[2], I. Poulios[2], and S. Sotiropoulos*[,2]

[1]Rostislaw Kaischew Institute of Physical Chemistry, Bulgarian Academy of Sciences, Sofia 1113, Bulgaria
[2]Department of Chemistry, Aristotle University of Thessaloniki, Thessaloniki 54124, Greece

***Abstract*:** Bi-layer WO_3/TiO_2 coatings, as well as single component WO_3 coatings, have been electrosynthesized on stainless steel 304 (SS) substrates from peroxytungstate and titanium oxosulfate acidic solutions by potentiostatic cathodic deposition. The resulting WO_3/TiO_2/SS and WO_3/SS photoelectrodes have been screened for their photoresponse under ultraviolet (UV) and visible (vis) light illumination by means of photovoltammetry and photoamperometry in sulfate solutions containing model organic pollutants. Larger specimens were also evaluated for bulk electrically enhanced photooxidation of oxalate and 4-chlorophenol under constant applied potential. It was found that the photoelectrocatalytic activity of bi-layer TiO_2/WO_3/SS is higher than that of plain WO_3/SS photoelectrodes under both UV and, most interestingly, VIS light illumination. This is interpreted by reduced electron-hole recombination rates due to electron transfer from TiO_2 to WO_3 (during UV light activation) and hole transfer from WO_3 to TiO_2 (during UV and vis light activation).

Introduction

Among other advanced oxidation technologies used in effluent treatment and environmental remediation, photocatalysis offers a promising solution for water detoxification that can, in principle, lead to complete organics mineralization (*1*, *2*). The most popular photocatalyst is crystalline TiO_2, a wide gap n-type semiconductor (*3*), activated by UV light (*3*) from solar or artificial radiation sources and used either in a slurry or supported layer form. There are two main targets of research aiming at improving the efficiency of TiO_2-based photocatalysts: minimizing photogenerated electron-hole recombination rates and expanding their useful range of operation into visible light wavelengths. Doping or mixing TiO_2 with appropriate compounds is a common strategy for achieving both targets. For example, doping with lanthanide ions (*4-6*) or coupling with WO_3 (*7-15*) are known to suppress electron-hole recombination rates. On the other hand, dye-sensitization (see for example Reference (*16*)) or, again, introduction of a visible light active catalyst such as WO_3 (*7-10*, *17-21*), improve visible light utilization. An alternative strategy to reduce recombination rates, applicable to photocatalyst films supported on conducting substrates, is that of electrically enhanced photocatalysis (22-24) whereby a positive bias is applied on the photocatalyst (in an appropriate electrochemical cell) and photogenerated electrons are drawn away from its surface through the external cell circuit.

Usually, particulate TiO_2 film preparation is carried out by dip-coating, spraying or sedimentation techniques (*25-27*) from suspensions of TiO_2 powder (either commercially available, such as Degussa P-25®, or prepared in the laboratory by sol-gel (*28-30*), hydrothermal (*31*, *32*) or spray-pyrolysis (*33*, *34*) methods). Electrosynthesis/electrodeposition has been proposed as an alternative route for the production of photocatalytic TiO_2 or/and WO_3-coated electrodes, on Pt, Au or optically transparent electrodes (*9-12*, *14*, *35*, *36*) and more recently on economical stainless steel (SS) substrates too (*15*, *37*, *38*). It offers the advantages of a cheap, one-step method, capable of coating substrates of various geometries.

In a recent series of papers we have used all three approaches mentioned above: coupling WO_3 with TiO_2, preparing the bi-layer catalyst by electrodeposition/ electrosynthesis and enhancing the photocatalytic rate by applying a positive bias (*15*, *38*). We have found that, not only were the UV light-generated photocurrents at the bi-layer WO_3/TiO_2 electrodes enhanced with respect to those observed at their plain WO_3 and TiO_2 analogues (as already reported for many other bi-component WO_3-TiO_2 systems (*7-12*, *14*)) but, most interestingly, the visible light-generated photocurrents were higher at the bi-layer electrodes than at the plain WO_3 ones. These photocurrent trends were translated into photooxidation trends during the bulk photoelectrolysis of a typical dye (malachite green) (*15*).

Keywords: tungsten trioxide coatings, titanium dioxide coatings, stainless steel, photoelectrochemistry, photooxidation

*Corresponding author;
E-mail address: eczss@chem.auth.gr ; eczss@otenet.gr
Tel.: +30 2310 997742; Fax: +30 2310 443922

The aim of this paper is to investigate whether the enhancement of the photoelectrocatalytic activity of electrosynthesized bi-layer TiO_2/WO_3-SS photoelectrodes with respect to their plain WO_3-SS analogues under UV and (mainly) visible light illumination, also holds for other typical organics too and can thus be of practical use. The main objectives are: *i.* To test the synthesised electrodes by photovoltammetry in solutions containing the model organic compound of oxalate and the typical contaminant of 4-chlorophenol (4-CP) and *ii.* To evaluate the photoelectrocatalytic activity of such photoelectrodes in oxalate and CP photooxidation under UV and vis light illumination, by constant potential bulk photoelectrolysis.

Experimental

a. WO_3 Electrodeposition and Bi-layer TiO_2/WO_3 Electrosynthesis/Electrodeposition on Stainless Steel (SS) Substrates

Small photoelectrode samples for photovoltammetry experiments were prepared in a small 300 ml three-electrode cell on stainless steel (SS) 304 plate small rectangular specimens (Silko-Inox; sample area 3 cm^2), using a Pt coil as the counter electrode. Larger samples (3cm x10cm) for bulk photoelectrolysis were prepared in a 2 L three-electrode cell with platinized titanium plate counter electrodes. As a reference electrode, we employed a mercurous sulfate $Hg/Hg_2SO_4/H_2SO_4$ (0.5M) electrode (MSE). An Autolab 30 potentiostat (EcoChimie) with a 20 A booster was used for electrodeposition/electrosynthesis. SS specimens were degreased with acetone and etched in a 1÷1 HCl/H_2O mixture for 60 s before the electrochemical preparation of the coatings.

The WO_3 layer on SS was formed by direct cathodic deposition (*15, 38*) for 30 min at –1.00 V vs. MSE, from a bath of pH=1.4 containing 0.025 M Na_2WO_4 ($Na_2WO_4.2H_2O$; Merck; pro analysi; >99%), 0.03 M H_2O_2 (30% aqueous solution) and 0.05 M HNO_3 (Riedel, 65%). After heating the resulting deposits at 350 °C for 30 min in air, crystalline WO_3 (monoclinic, as confirmed by XRD) was obtained. The small photoelectrode tested in this work had a WO_3 loading of 0.70 mg/cm^2 while that of the large sample had a 0.83 mg/cm^2 loading. TiO_2 layers were electrosynthesized on top of the already formed WO_3 layers by keeping the WO_3/SS electrode at -2.00 V vs. MSE for 30 min, from a solution of pH=1.4 containing 0.02 M $TiOSO_4$ (Fluka; Assay of Ti (as TiO_2) techn., >29%), 0.03 M H_2O_2 (30% aqueous solution), 0.05 M HNO_3 (Riedel, 65%) and 0.1 M KNO_3 (Merck, pro analysi, >99%) (*15, 37, 38*). The deposited gel films were heated in air at 400 °C for 1h to obtain crystalline TiO_2 (anatase, as confirmed by XRD) film. TiO_2 loadings were 0.20 mg/cm^2 for the small photoelectrode and 0.29 mg/cm^2 for the large specimens (loadings were determined by weighing the samples prior and after each deposition step).

b. Microscopic/EDS and XRD Characterisation of Coatings

Scanning Electron Microscopy (SEM) was carried out using a JSM 733 microscope equipped with an EDS facility. X-Ray Diffraction (XRD) deposit characterisation was performed with the help of a DRON automatic powder diffractometer (Bragg-Brentano arrangement, fixed slit mode) using Cu Kα filtered radiation and scintillation registration.

c. Photoelectrochemical Characterisation of Coatings

Photovoltammetry at small photoelectrodes was carried out with the Autolab 100 (EcoChimie) system, in a three-electrode cell equipped with a flat quartz window opposite the working electrode. The backside of the specimen (not facing the window) was insulated with epoxy resin so as not to contribute to the dark current. A saturated calomel electrode (SCE) was used as the reference electrode and a Pt foil as the counter electrode. Voltammograms were run for at least two consecutive times since preliminary experiments showed that a near-steady state response was observed only after the second cycle; all results reported correspond to the stabilized voltammetric picture.

In oxalate and 4-CP photoelectrolysis experiments a 500 ml cylindrical cell with a removable cap has been used. The UV or vis light lamp, placed in a cylindrical sleeve, was introduced from an opening in the middle of the cap leaving a solution available volume of 300 ml (filled with 250 ml of the 0.001 M oxalate or 4-CP solution to be treated). Samples of 2 ml were taken with the help of a tubing adjusted to a pipette. Oxalate was determined by permanganate titration. 4-CP was determined by spectrophotometry from the variation of the peak height at λ_{max}=280 nm. The fact that there was a continuous decrease of peak height and no change in peak shape or position during photoelectrolysis indicates that, unlike the case of Degussa P-25 ® TiO_2 (*39*), no significant quantities of quinone intermediates (known to interfere with the 4-CP spectrum) are formed at our WO_3 and TiO_2/WO_3 electrosynthesized/electrodeposited coatings, allowing the quantitative determination of 4-CP change at 280 nm. The rectangular (3cm x 10cm) electrodes were

suspended from the cell cap and touched the cell wall leaving a 0.5 cm gap between the front electrode surface and the lamp sleeve and being at a 2.5 cm distance from the lamp (the backside of all electrodes was covered with a layer of insulating epoxy resin glue). A stainless steel wire was used as the counter electrode and the reference electrode was a SCE electrode equipped with a salt bridge made of a thin thermoplastic tube ending to a Vycor® tip. The end of the tube was placed close to the upper edge of the photoelectrode to avoid obstruction of the incident light. A laboratory- made potentiostat was used for voltage application and current recording, interfaced to a PC for data collection via an18-bit AD card (Duo 18, WPI Inc.). Magnetic stirring was employed (at a stirring rate in the range where photo-degradation was found to be independent of stirring).

K_2SO_4 (Merck, pro analysi, >99%) or Na_2SO_4 (Merck, pro analysi, >99%) were used as supporting electrolytes (no significant dependence of the results on cation type was observed). Potassium oxalate (Fluka, >99.5%) and 4-chlorophenol (Fluka, >98% (GC)) were the model organic pollutants. Doubly distilled water was used for the preparation of solutions.

A Radium Ralutec 9W/78 UVA lamp (λ=350-400 nm, λ_{max}=366 nm), placed at a distance of 2.5 cm from the samples, was used for front face electrode illumination. The power density at the sample surface position was measured as 3 mW cm^{-2} with a photo-meter. A Radium Ralutec 9W/71 visible light lamp (λ>400 nm) was used in corresponding experiments.

Results and Discussion

a. Microscopic Characterisation of Coatings

Figures 1(A) and (B) show SEM micrographs of a WO_3 coating (0.83 mg cm^{-2} loading) electro-synthesized on SS. A "cracked-mud" morphology is observed, characterized by 5-30 μm large patches-islands separated by cracks. Closer inspection of the islands reveals some nodular features and surface microroughness (Figure 1(B)). EDS analysis (see below) and AES analysis (*38*) has shown that WO_3 is present also in the cracks, forming a thin film which is defective at locations (see for example a "hole" in the center of Figure 1(B)).

Figures 2(A) and (B) show SEM micrographs of a TiO_2/WO_3 bi-layer coating (0.29 mg cm^{-2} TiO_2/ 0.71 mg cm^{-2} WO_3 loading). The "cracked-mud" morphology of the first WO_3 layer is retained but the coating is now thicker. Although the terraces of the islands are smoothened by the presence of a TiO_2 overlayer these are also decorated by sparse nano-

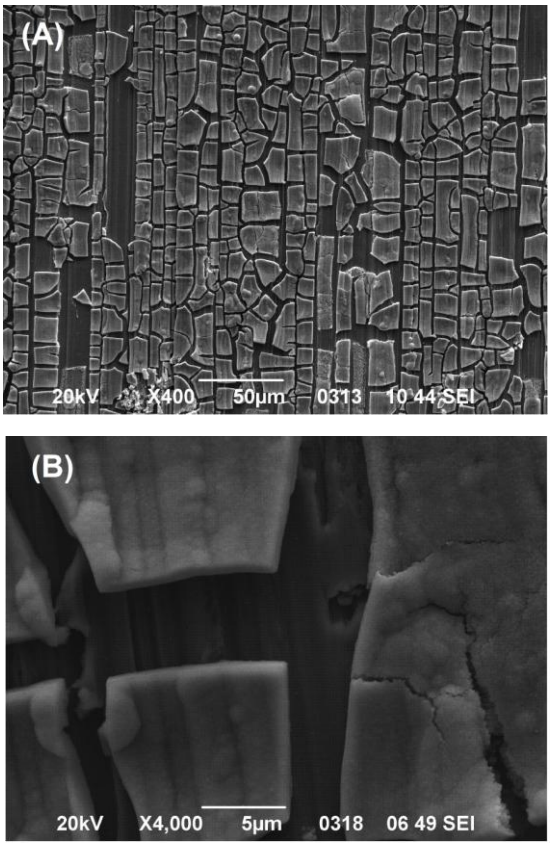

Figure 1. SEM micrographs of *(A)-(B)* a plain WO_3 coating, formed on a 304 stainless steel (SS) substrate.

particles. Figures 2(C) and (D) present the W and Ti elemental X-ray mapping obtained by EDS. It can be seen that there is extensive mixing of WO_3 and TiO_2 (necessary for successful synergism) and that TiO_2 pertains on island surfaces whereas WO3 dominates within the cracks (see the tilted "Y" region in the top-right-hand corner of Figures 2(B)-(D)).

b. Photoelectrochemical Characterisation of Coatings

b.1 Photovoltammetry Experiments

Figures 2 (A) and (B) show photovoltammo-grams (recorded at a 10 mV s^{-1} potential sweep rate towards positive potentials) of WO_3 (0.70 mg cm^{-2})/SS and TiO_2 (0.20 mg cm^{-2})/WO_3 (0.80 mg cm^{-2})/SS photoelectrodes respectively, under UV illumination in 0.1 M Na_2SO_4 solutions with and without 0.001 M oxalate or 4-chlorophenol. The shape of the curves is typical of n-type semiconductor behaviour with currents tending to a limiting value at sufficiently positive potentials due to minority charge carrier transport control. Since plots of the square of photocurrent vs. applied potential at the foot of the waves were found to be linear (*38*) (in accordance with the Gardner

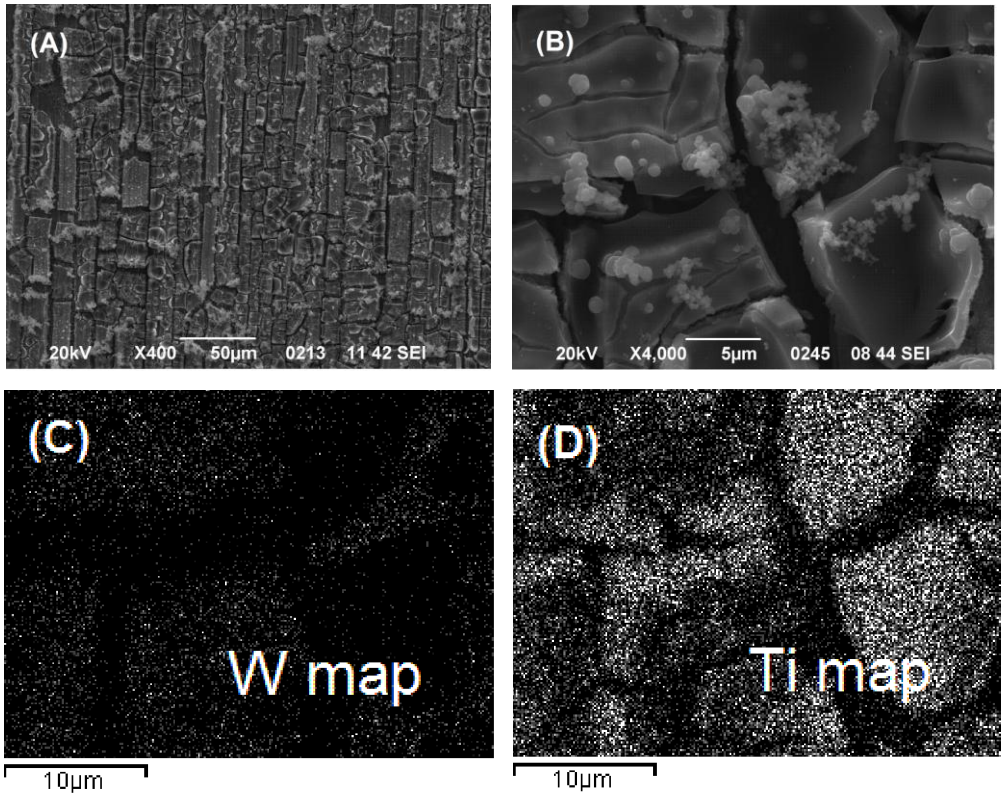

Figure 2. SEM micrographs of *(A)-(B)* a bi-layer TiO_2/WO_3 coating, formed on a 304 stainless steel (SS) substrates. EDS X-ray mapping of W *(C)* and Ti *(D)* at the area pictured in *(B)*.

model for semiconductor electrodes (*40*) and the resulting Butler equation [41]), the islands of the semiconductor deposits must be thick enough for a depletion layer to be formed. One may notice that the effect of chlorophenol on the photocurrent is insignificant, indicating that this species is not an efficient direct hole scavenger but instead it undergoes indirect photooxidation by $OH^{\bullet}$ radicals produced by hole scavenging by water molecules (*10*, *42*, *43*). On the other hand, the addition of oxalate results in a large photocurrent enhancement, characteristic of direct hole scavenging by oxalate which is further enhanced by the "current doubling" effect whereby electron injection by the initial oxidation product to the conduction band of the photocatalyst takes place (*44*, *45*). The enhancement of the photocurrent when passing from supporting electrolyte (sulfate solution) to oxalate solutions, is more pronounced in the case of the plain WO_3/SS electrode, indicating that the recombination rates are higher at this material than at the bilayer TiO_2/WO_3 one, making the need of an effective hole scavenger more important. To further quantify the UV photoactivity of the two types of electrodes in different media, the incident photon-to-current efficiencies (IPCEs; given by IPCE%=100 x (1240 i_{ph} / λP) (*46*), where i_{ph} is the photocurrent at +0.7 V vs. SCE in mA cm^{-2}, λ the wavelength of the incident light in nm and P the incident light intensity in mW cm^{-2}) are given in Table 1. These values are in the range of values reported for micro-particulate TiO_2 electrodes in other studies (*47*, *48*).

Table 1. Incident photon-to-current efficiency (IPCE, %) of WO_3/SS and TiO_2/WO_3/SS photoelectrodes under UV light illumination in 0.1 M sulfate solutions with and without 10^{-3} M oxalate and 4-chlorophenol (4-CP).

	UV light		
	sulphate	**4-CP**	**oxalate**
WO_3/SS	5.99	8.73	55.46
TiO_2/WO_3/SS	19.86	25.26	53.27

Figures 4(A) and (B) show photovoltammograms of plain and bi-layer samples in the same solutions but under visible light (vis) illumination (λ>400 nm). Similar trends to those observed for UV light are observed. Finally, Figures 5(A) and (B) provide a direct comparison of the photovoltammograms characterizing the two different materials under either UV or visible light illumination, in oxalate and chlorophenol solutions respectively. In the case of the effective oxalate scavenger, there is no significant difference in photocurrents under UV illumination and only a moderate enhancement under visible light illumination when

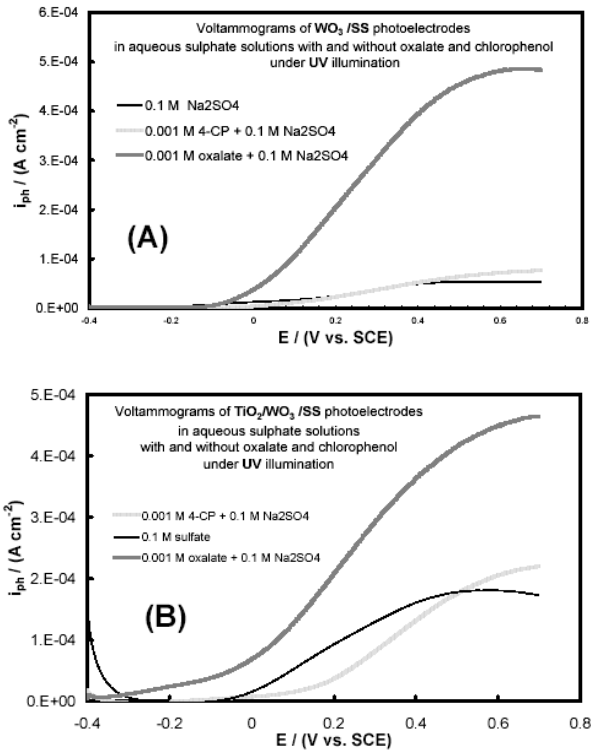

Figure 3. Photovoltammograms (10 mV s^{-1} potential scan rate; positive going sweep) at WO_3/SS *(A)* and TiO_2/WO_3/SS *(B)* electrodes in 0.1 M Na_2SO_4 + 10^{-3} M oxalate or 4-chlorophenol solutions, under UV illumination.

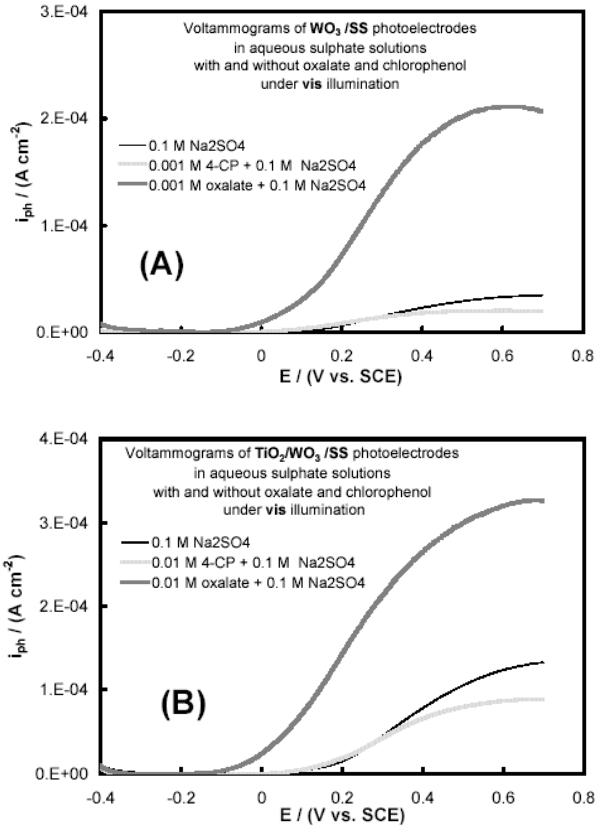

Figure 4. Same as in Figure 3 but for visible light (vis) illumination.

one passes from plain to bi-layer samples (Figure 5(A)). In the case of 4-chlorophenol which is more difficult to oxidize and, due to its indirect oxidation mechanism, does not limit recombination rates, the TiO_2/WO_3 combination has a pronounced effect in increasing the photocurrent (Figure 5(B)).

A reduction in electron-hole recombination rates TiO_2/WO_3 bi-component systems under UV illumination (and the corresponding photocurrent increase) could result from the mismatch of the E_g=3.2 eV energy gap of anatase (*3*) with that of the indirect type excitation gap of E_g=2.7-2.8 eV of WO_3 (*8*), and the resulting electron injection from TiO_2 to WO_3 and hole injection in the opposite direction, as shown in the valence and conduction band energy diagrams of Figure 6(A). However, the significant enhancement of visible light photoactivity of the bi-layer samples when compared to plain WO_3 is at a first glance unexpected since the TiO_2 overlayer cannot be activated on its own to a significant extent by visible light illumination. Efficient visible light absorbance by WO_3 can then only be considered if either the TiO_2 overlayer is thin enough to be transparent to visible light or microporous (at least at locations). AES analysis (*15*) and EDS X-ray mapping (see above) do not exclude these possibilities. Once the underlying or neighbouring WO_3 is photoactivated by visible light then its photogenerated holes are transferred to the valence band of TiO_2, where they oxidise water to $OH^{\bullet}$ at the electrode surface (see energy diagram of Figure 6(B)). An equivalent representation of the situation, perhaps more appropriate since TiO_2 has no significant semiconductor conductivity under visible light illumination, may be the equivalent electron transfer from the TiO_2 valence band to WO_3 with simultaneous electron transfer from solution oxidisable species to TiO_2.

b.2 Photoelectrolysis Experiments

In order to compare the efficiency of the WO_3-TiO_2/SS and WO_3/SS photoelectrodes towards the photooxidation of oxalate and 4-CP, we carried out constant potential bulk photoelectrocatalytic experiments, using electrodes in the 30 cm^2 range and 250 ml 0.1 M Na_2SO_4 +10^{-3} M oxalate or 4-CP solutions. The potential was kept constant at +0.4 V vs. SCE. To study the effect of applied potential we also performed the experiments without the application of an external bias. Figures 7 and 8 present results for oxalate and 4-CP, under UV (A) or visible (B) light illumination, in the presence or absence of a bias.

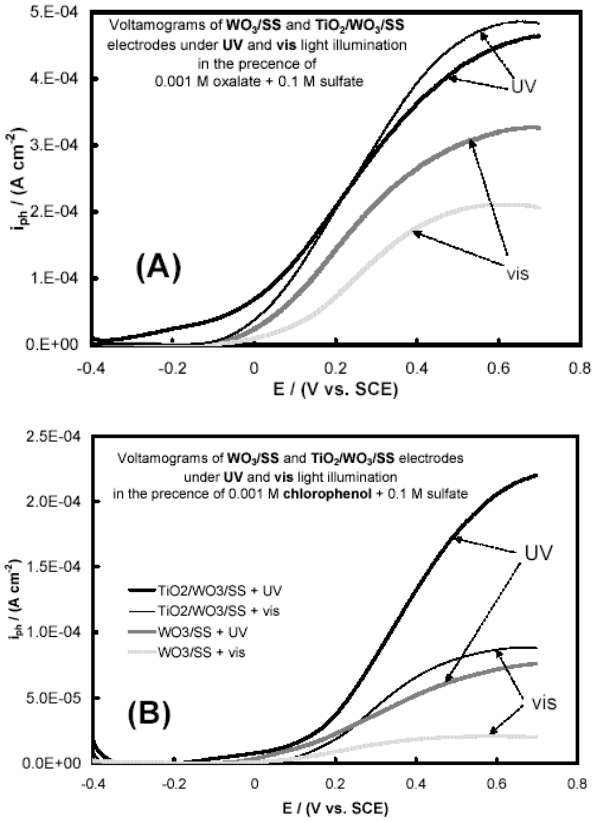

Figure 5. Comparison of photovoltammograms (10 mV s^{-1} potential scan rate; positive going sweep) at WO_3/SS and TiO_2/WO_3/SS electrodes under UV or visible light illumination in 0.1 M Na_2SO_4 + 10^{-3} M oxalate (A) and 4-chlorophenol (B) solutions.

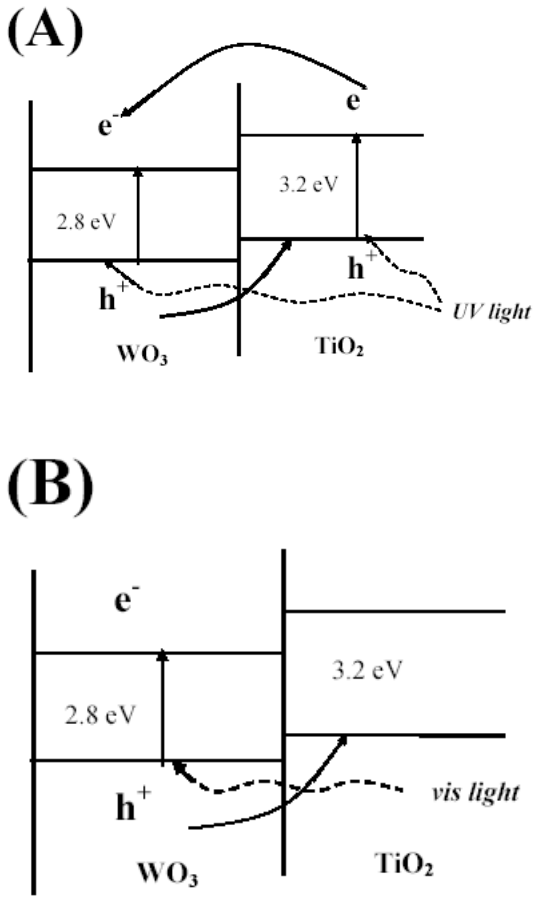

Figure 6. Energy diagram of WO_3 and TiO_2 materials in contact, showing corresponding valence and conduction band positions as well as hole and electron transfer, during UV (A) and visible (B) light illumination.

Two general remarks can be readily made. First, there is a pronounced beneficial effect of the applied potential on the photocatalytic activity of both materials. This is important for the effective use of supported photocatalysts since, when compared to their slurry analogues, they have a limited surface area and are prone to mass transport limitations. It becomes even more critical in the case of the coatings prepared in this work, since they are not micro-particulate as typical TiO_2 layers prepared from powder catalysts and hence they posses a relatively smaller area. Second, the trends reported and interpreted above for the photocurrents at the plain and bi-layer samples are in general translated into similar trends for the photoelectrocatalytic oxidation of oxalate and CP. That is, the bi-layer TiO_2/WO_3/SS photoelectrodes exhibit in all cases superior organics degradation performance when compared to plain WO_3/SS photoelectrodes.

To quantify the efficient use of the photocurrent for the degradation of organics we have also estimated the faradaic efficiency of oxalate and 4-CP removal at the TiO_2/WO_3/SS and WO_3/SS electrodes, under UV and visible light illumination. This was done by calculating the charge passed during the reaction period (by integrating the corresponding photocurrent vs. time curves) and comparing it with the charge associated to the photooxidation of these species (estimated by their actual concentration change and applying Faraday's law). The faradaic efficiency represents that part of the photocurrent which is used for the organics oxidation. The results are presented in Table 2. It can be seen that despite the fact that the bi-layer TiO_2/WO_3 electrodes are more active than WO_3 in removing both oxalate and 4-chlorophenol (Figures 7 and 8 as discussed above), the plain WO_3 electrodes are characterized by a more effective use of the photocurrent. This in turn means that at TiO_2/WO_3 electrodes the rate of concurrent reactions (such as oxygen evolution from the reaction of $OH^{\bullet}$ radicals with each other) is higher. Also, the faradaic efficiency in the case of oxalate photooxidation is higher than that of 4-chlorophenol, since the former reaction may not involve the generation $OH^{\bullet}$ radicals but instead direct scavenging of photogenerated holes.

Table 2. Faradaic efficiency (%) of WO_3/SS and TiO_2/WO_3/SS photoelectrodes in photoelectrocatalytic degradation of 10^{-3} M oxalate and 4-chlorophenol (4-CP), under UV and visible light illumination.

	UV light		*Visible light*	
	oxalate	**4-CP**	**oxalate**	**4-CP**
WO_3/SS	109	34	73	68
TiO_2/WO_3/SS	89	23	73	34

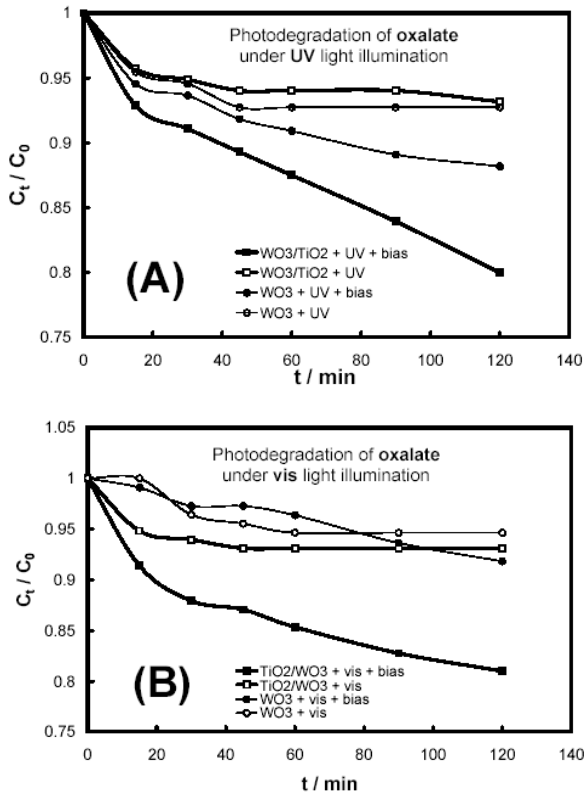

Figure 7. Variation of oxalate concentration with time from 10^{-3} M oxalate + 0.1 M Na_2SO_4 250 ml solutions, during constant potential (+0.4 V vs. SCE) photoelectrolysis at large (30 cm^2) WO_3/SS and TiO_2-WO_3/SS electrodes, under UV *(A)* and visible *(B)* light illumination.

Conclusions

(i) Bi-layer TiO_2/WO_3 coatings prepared by cathodic electrosynthesis/electrodeposition on stainless steel 304 (SS) substrates exhibited in general higher photocurrents than plain single layer WO_3 coatings, both under UV and visible light illumination when used as photo-electrodes in supporting electrolyte (sulphate) solutions. The enhancement of UV photocurrents at TiO_2-WO_3 electrodes is interpreted by reduced recombination rates at both materials while that of vis photocurrents by WO_3 excitation and transfer of its holes to a thin and/or prous TiO_2 overlayer.

(ii) In the presence of the model organic species of oxalate which acts as a direct hole scavenger and also

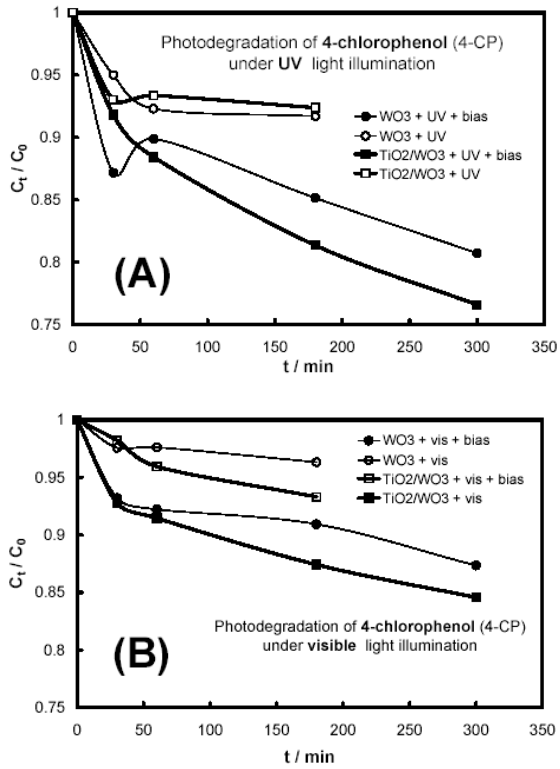

Figure 8. Variation of 4-chlorophenol concentration with time from 10^{-3} M 4-chlorophenol + 0.1 M Na_2SO_4 250 ml solutions, during constant potential (+0.4 V vs. SCE) photoelectrolysis at large (30 cm^2) WO_3/SS and TiO_2-WO_3/SS electrodes, under UV *(A)* and visible *(B)* light illumination.

exhibits a current doubling effect, there is significant enhancement of the photocurrents when compared to their values in plain supporting electrolyte solutions. On the contrary, 4-chlorophenol does not increase the photocurrent, indicating that it undergoes indirect oxidation by OH radicals produced by the reaction of photogenerated holes with water.

(iii) The application of an external bias (instead of operating the reactor in an open-circuit, photocatalytic mode) and the use of bi-layer TiO_2-WO_3/SS photo-electrodes (instead of single layer WO_3 ones) both improve condiderably the photooxidation of oxalate and 4-chlorophenol under UV and visible light illumination.

Acknowledgments

This work was supported by a NATO Science for Peace Project 982835.

References

(*1*) Hoffmann, M.R.; Martin, S.T.; Choi, W.; Bahnemann, D.W. *Chem.Rev.* **1995**, *95*, 69.

(*2*) Fujishima, A.; Rao, T.N.; Tryk, D.A. *J. Photochem. Photobiol. C: Photochem. Rev.* **2000**, *1*, 1.

(*3*) H.O.Finklea (Ed.), *Semiconductor Electrodes*, Elsevier, Amsterdam, 1998.

(*4*) Ranjit, K.T.; Willner, I.; Bossmann, S.H.; Braun, A.M. *J. Catal.* **2001**, *204*, 305.

(*5*) Li, F.B.; Li, X.Z.; Ao, C.H.; Lee, S.C.; Hou, M.F. *Chemosphere* **2005**, *59*, 787.

(*6*) Uzunova, M.; Konstantinov, M.; Georgieva, J.; Dushkin, C.; Todorovsky, D.; Philippidis, N.; Poulios, I.; Sotiropoulos, S. *Appl. Catal. B.* **2007**, *73*(1-2), 23.

(*7*) He, T.; Ma, Y.; Cao, Y.; Hu, X.; Liu, H.; Zhang, G.; Yang, W.; Yao, J. *J.Phys.Chem. B.* **2002**, *106*, 12670.

(*8*) Miyauchi, M.; Nakajima, A.; Watanabe, T.; Hashimoto, K. *Chem.Mater.* **2002**, *14*, 4714.

(*9*) Shiyanovskaya, I.; Hepel, M. *J. Electrochem. Soc*. **1999**, *146*, 243.

(*10*) Luo, J.; Hepel, M. *Electrochim. Acta*. **2001**, *46*, 2913.

(*11*) Chenthamarakshan, C.R.; de Tacconi, N.R.; Rajeshwar, K.; Shiratsuchi, R. *Electrochem. Commun.* **2002**, *4*, 871.

(*12*) de Tacconi, N.R.; Chenthamarakshan, C.R.; Rajeshwar, K.; Pauporte, T.; Lincot, D. *Electrochem.Commun.* **2003**, *5*, 230.

(*13*) Georgieva, J.; Armyanov, S.; Valova, E.; Tsacheva, Ts.; Poulios, I.; Sotiropoulos, S. *J. Electroanal. Chem.* **2005**, *585*, 35.

(*14*) Somasundaram, S.; Chenthamarakshan, C.R.; de Tacconi, N.R.; Basit, N.A.; Rajeshwar, K. *Electrochem. Commun.* **2006**, *8*(4), 539.

(*15*) Georgieva, J.; Armyanov, S,; Valova, E.; Poulios, I.; Sotiropoulos, S. *Electrochemistry Communications* **2007**, *9*, 365-370.

(*16*) O'Regan, B.; Gratzel, M. *Nature (London)* **1991**, *353*, 737.

(*17*) Bostt, M; Jansses, F. *Catal.Today* **1998**, *2*, 429.

(*18*) Gillet, M.; Aguir, K.; Lemire, C.; Gillet, E.; Schierbaum, K. *Thin Solid Films* **2004**, *467*, 239.

(*19*) Kopp, L.; Harmon, B.N.; Liu, S.H. *Solid State Commun.* **1977**, *22*, 677.

(*20*) Ohno, T.; Tanigawa, F.; Fujihara, K.; Izumi, S.; Matsumura, M. *J.Photochem.Photobiol.A: Chem.* **1998**, *118*, 41.

(*21*) Santato, C.; Ulmann, M.; Augustynski, J. *J. Phys. Chem. B.* **2001**, *105*, 936.

(*22*) Butterfield, I.M.; Christensen, P.A.; Hamnett, A.; Shaw, K.E.; Walker, G.M.; Walker, S.A.; Howarth, C.R. *J. Appl. Electrochem.* **1997**, *27*, 385.

(*23*) Candal, R.J.; Zeltner, W.A.; Anderson, M.A. *J. Adv. Oxid. Technol.* **1998**, *3*(3), 270.

(*24*) Fernandez-Ibanez, P.; Malato, S.; Enea, O. *Catal. Today* **1999**, *54*, 329.

(*25*) Peill, N.J.; Hoffmann, M.R. *Environ. Sci. Technol.* **1995**, *29*, 2974.

(*26*) Byrne, J.A.; Eggins, B.R.; Brown, N.M.D.; McKinney, B.; Rouse, M. *Appl. Catal. B:Environmental* **1998**, *17*, 25.

(*27*) Krysa, J.; Jirkovsky, J. *J. Appl. Electrochem.* **2002**, *32*, 591.

(*28*) Takahashi, Y.; Matsuoka, Y. *J. Mater. Sci.* **1988**, *23*, 2259.

(*29*) O'Regan, B.; Moser, J.; Anderson, M.; Gratzel, M. *J. Phys. Chem.* **1990**, *94*, 8720.

(*30*) Kato, K.; Tsuzuki, A.; Torii, Y.; Taoda, H.; Kato, T.; Butsugan, Y. *J. Mater. Sci.* **1995**, *30*, 837.

(*31*) Shin, H.; Collins, R.J.; DeGurie, M.R.; Heuer, A.H.; Sukenik, C.M. *J. Mater. Res.* **1995**, *10*, 692.

(*32*) Langlet, M.; Kim, A.; Audier, M.; Guillard, C.; Herrmann, J.M. *J. Mater. Sci.* **2003**, *38*, 3945.

(*33*) Kavan, L.; Gratzel, M. *Electrochim. Acta*. **1995**, *40*, 643.

(*34*) Martinez, A.I.; Acosta, D.R.; Lopez, A.A. *J. Phys.: Condens. Matter* **2004**, *16*, S2335.

(*35*) Natarajan, C.; Nogami, G. *J. Electrochem. Soc.* **1996**, *143*, 1547.

(*36*) Hepel, M.; Hazelton, S. *Electrochim. Acta.* **2005**, *50*(25-26), 5278.

(*37*) Georgieva, J.; Armyanov, S.; Valova, E.; Poulios, I.; Sotiropoulos, S. *Electrochim. Acta*. **2006**, *51*, 2076.

(*38*) Georgieva, J.; Armyanov, S.; Valova, E.; Tsacheva, Ts.; Poulios, I.; Sotiropoulos, S. *J. Electroanal. Chem.* **2005**, *585*, 35.

(*39*) Gu Kang, M.; Han, H.-E.; Kim, K.-J. *J. Photochem. Photobiol. A: Chem.* **1999**, *125*, 119.

(*40*) Gardner, W.W. *Phys. Rev.* **1959**, *116*, 84.

(*41*) Butler, M.A. *J. Appl. Phys.* **1977**, *48*, 19.

(*42*) Takahashi, Y.; Matsuoka, Y. *J. Mater. Sci.* **1988**, *23*, 2259.

(*43*) Hepel, M.; Hazelton, S. *Electrochim. Acta*. **2005**, *50*(25-26), 5278.

(*44*) Calvo, M.E.; Candal, R.J.; Bilmes, S.A.; *Environ. Sci. Technol.* **2001**, *35*, 4132.

(*45*) Villareal, T.L.; Gomez, R.; Neumann-Spallart, M.; Allonso-Vante, N.; Salvador, P. *J. Phys. Chem. B.* **2004**, *108*, 15172.

(*46*) Vinodgopal, K.; Stafford, U.; Gray, K.A.; Kamat, P.V. *J. Phys. Chem.* **1994**, *98*, 6797.

(*47*) Waldner, G.; Pourmodjib, M.; Bauer, R.; Neumann-Spallart, M. *Chemosphere* **2003**, *50*, 989.

(*48*) Krysa, J.; Keppert, M.; Waldner, G.; Jirkovsky, J. *Electrochim. Acta*. **2005**, XX, XX.

Received for review March 15, 2008. Revised manuscript received April 30, 2008. Accepted April 30, 2008.